Photocatalytic Degradation of Bisphenol A (BPA) Present in Aqueous Solution Using g-C₃N₄ Nanosheets Under Solar Light Irradiation

Faisal Al-Marzouqi [1,2] and Rengaraj Selvaraj[1]*

*[1]Department of Chemistry, Sultan Qaboos University, P.O. Box 36, P.C. 123, Al-Khoudh, Muscat, Sultanate of Oman; [2]Department of Process Engineering, International Maritime College Oman, P.O. Box 532, PC 322, Falaj Al Qabail, Suhar, Oman.,*E-mail: rengaraj@squ.edu.om.*

ABSTRACT: A graphite-like carbon nitride (g-C₃N₄) nanosheet sample was synthesized from a melamine precursor by a method of simple direct heating in a semi-closed system followed by thermal oxidation etching at 550 °C for 12 h. The sample was labelled as (g-C₃N₄12h) and was systematically characterized. Moreover, the results were then compared with a pristine g-C₃N₄ sample for the degradation of Bisphenol A (BPA) present in water. Bisphenol A (BPA) is an endocrine disruptor. It is known that the BPA is one of the most harmful organic materials and that it does not degrade easily in the environment. It was therefore selected as a target to test the photocatalytic activity of prepared carbon nitride nanosheets under direct solar irradiation. The results showed the structure of the g-C₃N₄ nanosheets when the sample had been treated for a longer time compared to the regular treatment time. The optical band gap results remained the same, indicating the existence of a g-C₃N₄ backbone structure. However, the XPS and FTIR spectra showed some modification on g-C₃N₄ after longer etching treatment time such as the C-H, CO and N pyridinic structure. The photocatalytic degradation of Bisphenol A by the g-C₃N₄ nanosheets under solar irradiation was much better (around 60%) than that with the g-C₃N₄3h bulk sample (around 30%). This enhanced photocatalytic activity can be attributed to multiple factors such as the smaller particle size, rich carbon surface and high surface area exhibited by the g-C₃N₄ nanosheets. This further indicates that g-C₃N₄ can be used with solar irradiation to treat wastewater containing endocrine disruptor chemicals.

Keywords: Bisphenol A; Carbon Nitride; Graphite; Nanosheet; Photocatalyst.

التكسير التحفيزي الضوئي للبيسينفول أ (BPA) باستخدام شرائح نانومترية من الكربون المنترد g-C₃N₄ تحت إشعاع ضوء الشمس المباشر

فيصل المرزوقي ورنجراج سلفراج

الملخص: تحضير عينات من شرائح الكربون المنترد g-C₃N₄ الشبيهة بالجرافين باستخدام المعالجة الحرارية المباشرة لمركب الميلامين في بوتقة شبه مغلقه. كان التحضير متبوعًا بالأكسدة الحرارية عند درجة 550 مئوية لمدة 12 ساعة لتحويل المادة الى شرائح نانومتريه صغيرة. تم دراسة العينات بشكل منهجي. حيث تمت مقارنة النتائج مع عينة g-C₃N₄ غير معالجة بالأكسدة الحرارية من حيث قوتها لتحطيم مركب بيسفينول أ Bisphenol A (BPA)الموجود في الماء. البيسفينول أ هو مادة معطلة لعمل الغدد الصماء ومن المعروف أن مادة BPA هي من أكثر المواد العضوية ضررًا ولا تتحلّل بسهولة في البيئة. لذلك، تم اختياره كهدف لاختبار النشاط التحفيزي لهذه الشرائح النانومترية بمساعدة الإشعاع شمسي المباشر. أظهرت النتائج ان العينات عندما عولجت لفترة أطول مقارنة بوقت العلاج المعتاد اكتسبت خصائص تحفيزية أكثر فعالية. حيث اكتسب العينة القدرة على فصل نواقل الشحنات لمدة أطول مقارنة بالعينة الغير معالجة،كما أظهر أطياف XPS و FTIR بعض التعديل على تركيب ال g-C₃N₄ بعد وقت معالجة أطول مثل وجود لكل من-C H و CO و N بيريدين. كان التحلل الضوئي لـ Bisphenol A بواسطة الصفائح g-C₃N₄ تحت الإشعاع الشمسي أفضل بكثير (حوالي 60 %) من ذلك مع العينة الغير معالجة بالأكسدة الحرارية (حوالي 30 %). يمكن أن يُعزى هذا التحسين على نشاط التحفيز الضوئي إلى عوامل متعددة مثل حجم الجسيمات الأصغر وسطح الغني بالكربون ومساحة السطح العالية التي تظهرها الشرائح النانومترية. ان هذه الدراسة تشير إلى أنه يمكن استخدام g-C₃N₄ لمعالجة مياه الصرف التي تحتوي على مواد كيميائية تؤدي إلى اختلال الغدد الصماء بمساعدة هذه المحفزات الضوئية والإشعاع الشمسي.

الكلمات المفتاحية: البيسفينول أ، الكربون المنترد، الجرافيت، شرائح نانومترية ، المحفزات الضوئية.

PHOTOCATALYTIC DEGRADATION OF BISPHENOL A (BPA)

Graphical Abstract
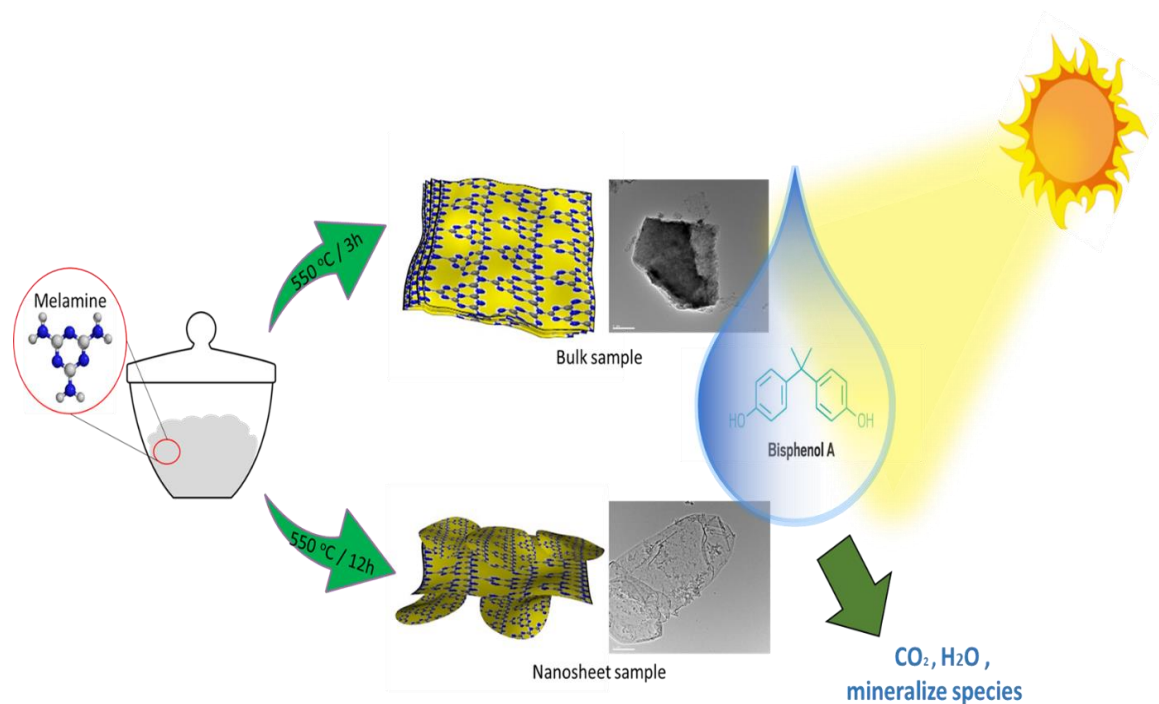
1. Introduction

Nowadays, a significant awareness has been established with regard to the impact on human health of the organic and inorganic contaminants in the water and environment. These toxic wastes are growing yearly in our environment due to both increased development and energy demand. Recently there have been more and more studies highlighting the presence of these chemical pollutants in water. There are many ways in which these contaminants can reach water bodies, as emphasized in much research [1-4]. Many organic pollutants have been found in the environment in levels of µg/L to ng/L. Amongst all the organic contamination, the pharmaceuticals and personal products and the endocrine disrupting chemicals have attracted more attention due to their potential risk to human health .[5] Furthermore, the polycarbonate resins and antioxidant materials used to stabilize plastics mainly depend on the use of Bisphenol A (BPA). BPA has been identified as an endocrine disrupting pollutant that changes the function of the endocrine system and consequently causes adverse effects in the health of an organism.[6] Thus developing efficient techniques to remove emerging contaminants from water and wastewater is a very urgent need.

The degradation of such pollutants using active photocatalysts is a promising technique to treat wastewater.[7] Several photocatalysts, such as metal oxides and metal sulphides have been applied for this purpose [8]. There is a growing awareness of visible active photocatalysts.[9,10] Unfortunately, most metal based material shows a weak light absorption, low stability and is of high price.[11-14] Recently, carbon based photocatalysts have emerged as promising conducting materials due to their high charge mobility. Carbon nitride (g-C_3N_4) is an interesting photocatalytic material. Wang *et al* and his co-worker have published regarding the use of bulk carbon nitride as an active photocatalyst for hydrogen development under irradiation with visible light.[15] A great deal of attention has focussed on the use of g-C_3N_4 for pollutant degradation and chemical synthesis. Most of these studies used bulk carbon nitride material. The carbon nitride (g-C_3N_4) constructed of nano sheets has a 2D polymer semiconductor structure that is very similar to that of graphene (Figure 1a). The band gap of this graphite like carbon nitride (g-C_3N_4) photocatalyst was measured to be around 2.7 eV[16-17]. The g-C_3N_4 has shown interesting properties including a suitable redox potential, a band structure located in the visible light region unlike the band structure of TiO_2 which is located in UV region (Figure 1b), thermal and chemical stability, and an ease of preparation that would allow for large-scale production from low-cost precursors.[18,19]

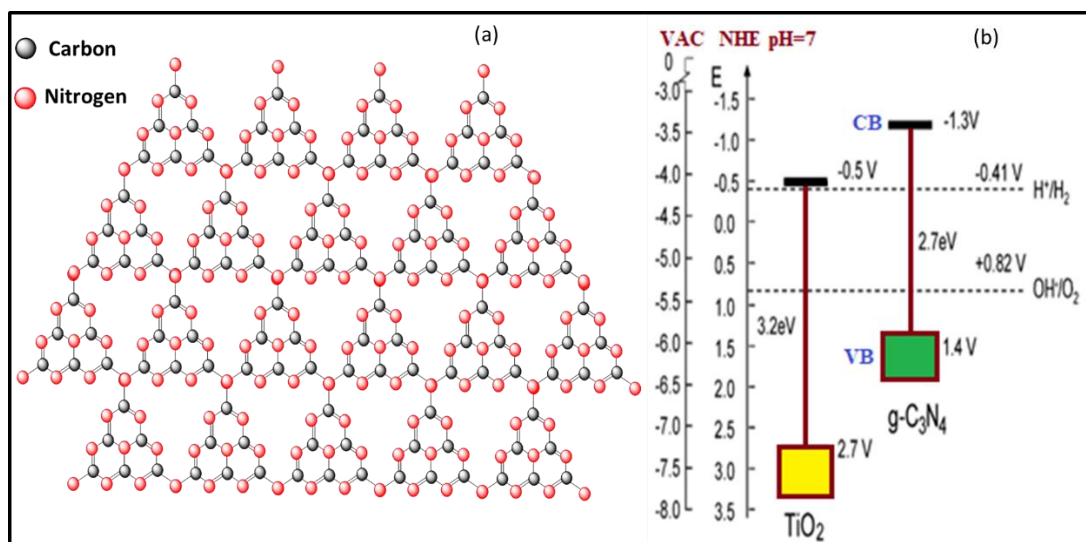**Figure 1.** (a) The chemical structure of graphite-like carbon nitride (g-C₃N₄) sheet and (b) the band gap structure comparison of graphite-like carbon nitride (g-C₃N₄) with titanium dioxide.

The carbon nitride (g-C₃N₄) semiconductor can be prepared via a thermal polycondensation process either in a low vacuum system or under high pressure.[20-22] Moreover, several research groups have successfully prepared carbon nitride (g-C₃N₄) under ambient pressure in a semi-closed system, which would be more convenient from an industrial point of view[23,24]. Unfortunately, the resulting product was a bulk carbon nitride material and its activity was considered insignificant. The transformation of g-C₃N₄ bulk material to nanosize can be achieved by different methods such as acidification and sonication[25]. The thermal oxidation process has been less investigated and therefore, enhancement of g-C₃N₄ photocatalytic performance is targeted to transfer the g-C₃N₄ bulk material to nanosize materials via this process. To enhance the degradation of Bisphenol A via g-C₃N₄ nanosheets obtained from g-C₃N₄ bulk materials via thermal oxidation process. The report here, pointed out an enhancement of the degradation of Bisphenol A with help of g-C₃N₄ nanosheets obtained from g-C₃N₄ bulk materials via thermal oxidation process under solar light irradiation.

2. Experimental section

2.1 Materials and preparation

The nitrogen rich precursor (melamine) was supplied by Sigma-Aldrich and was used in the synthesis of g-C₃N₄ without further purification. The preparation took place in a muffle furnace, where melamine powder was subjected to direct heating in a semi-closed system. A small amount of melamine powder (1g) was placed in a crucible with a cover. The direct heating increased the temperature from room temperature to 550 °C at a heating rate of 20 °C/min. the thermal etching process was conducted at 550 °C for 12 h, and the g-C₃N₄ nanosheets were obtained. (For comparison, 1 g of melamine powder was heated at 550 °C for 3 h to prepare the g-C₃N₄ bulk material.) The product was collected for further analysis.

2.2 Characterization

Crystal property was investigated by X-ray diffraction (XRD) analysis, using a benchtop X-ray diffractometer (MiniFlex600). The morphology was examined and elemental surface analysis (EDX) performed with a Transmitted Electron Microscope (TEM) of model (JEM-1400-JEOL, Japan). X-ray photoelectron spectroscopy (XPS) measurements were conducted using multi-probe X-ray photoelectron spectroscopy (XPS) (Omicron Nanotechnology, Germany). The results were analysed using the Casa XPS software (Casa Software Ltd). UV-vis diffuse reflection spectroscopy (UV-vis DRS) was performed on a UV-Vis Spectrometer Lambda 650S (Perkin Elmer), and the infrared spectra were obtained using CARY 600 FTIR (Agilent Technologies). Optical properties were investigated via photoluminance (PL) with the help of a PerkinElmer LS55 spectrometer. The particle sizes were measured using a Microtrac particle sizer. The surface analysis obtained by Brunauer Emmett Teller (BET) surface area analysis using ASAP2010 under liquid N₂ with 50 P/P₀ points, Micromeritics, USA.

2.3 Photocatalystic activity test

Bisphenol A (BPA) is an endocrine disruptor which was selected to be used for testing the photocatalytic activity of prepared nanosheet and pristine carbon nitride samples. All photoreaction experiments were carried out in a photocatalytic reactor batch system consisting of a cylindrical borosilicate glass reactor vessel with an effective volume of 500 ml. The activity studies were conducted in an open atmosphere with an air diffuser fixed at the reactor to

uniformly disperse the air into the solution. The reaction suspensions were prepared by adding 0.1 g of as-prepared g-C_3N_4 into 250 ml of aqueous bisphenol A (BPA) solution with an initial concentration of 10 mg/L. Prior to illumination, the reaction suspensions were magnetically stirred for 30 min in darkness to ensure adsorption-desorption equilibrium between the photocatalyst and the bisphenol A (BPA). During illumination (under solar light of average 1400 W/m^2), about 6 ml of the suspension solution were taken from the reactor at scheduled interval. The samples were centrifuged at 8000 revolutions per minute for 5 min and were then filtered to remove the catalyst. The filtrate was analysed using a Shimadzu1800 UV-vis spectrophotometer.

3. Results and discussion

3.1 Characterization of g-C_3N_4 nanosheets

The EDX analysis (Fig. 2a) revealed the presence of carbon (C) and nitrogen (N) as the main elements. A weak signal was detected from the platinum coating. This result indicates the high purity of the samples. The morphology of the samples showed a sheet structure, which is a characteristic shape of g-C_3N_4. TEM analysis (Fig2b and 2c) showed the clear transformation of the multilayer bulk structure (dark colour) to nanosheet structure (transparent colour).
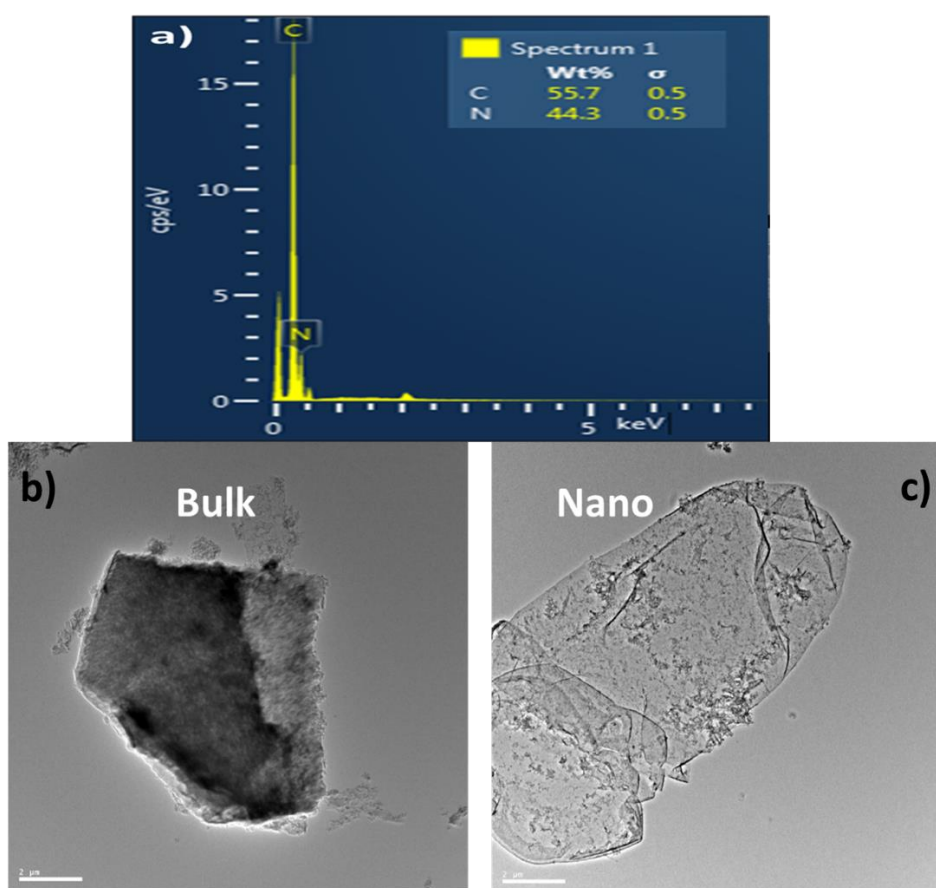

Figure 2. (a) EDX spectrum of g-C_3N_4 nanosheet and SEM image (b) and (c) TEM images of g-C_3N_4 bulk and nanosheet respectively.

The XRD results for the g-C_3N_4 samples are shown in Fig. 3. Carbon nitride materials exhibit two diffraction peaks at 27.90^o corresponding to the (002) plane typical for the interlayer stacking of the C-N conjugated aromatic systems and a peak at 13.05^o for the (100) plane and representing the interplanar separation of tri-s-triazine units. [28] The position of the diffraction peaks was retained during the treatment process, showing the existence of the main structure of g-C_3N_4. However, the overall diffraction intensity was reduced by increasing the etching treatment from three to up to 12 hours. The (001) plane peak disappeared after 12 h of treatment, and this can be considered to be a consequence of the reduced structural correlation length prompted by a decrease in the number of layers. This result reflects the formation process of the g-C_3N_4 nanosheets.
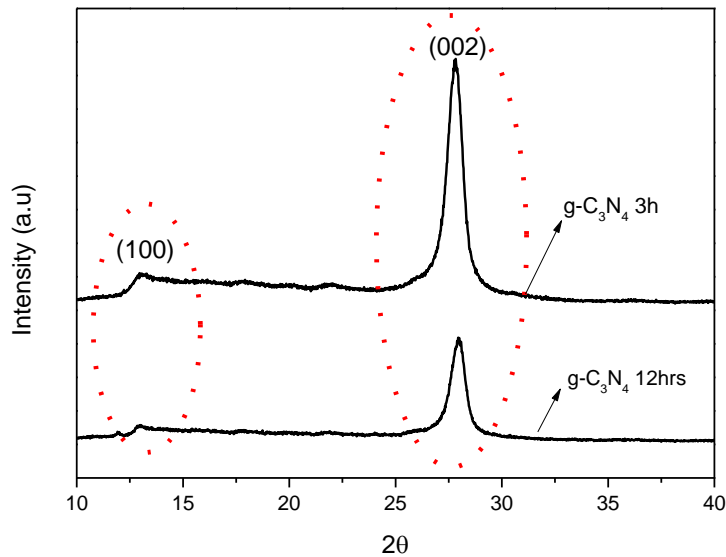
Figure 3. XRD patterns of g-C$_3$N$_4$ samples obtained after 3 and 12 h of heating.

Figure 4 presents the Fourier transform infrared (FTIR) spectrum of the as-prepared samples to identify the specific interaction of the functional groups. The result indicates the presence of the graphite-like structure of carbon nitride. The N-H stretching modes and the O-H from water absorbed on the surface are present in the broad peak observed in the range of 3000-3500 cm^{-1} (area 1). The bands around 1200-1600 cm^{-1} are characteristic of a typical stretching mode of CN heterocycles (area2). In addition, the s-triazine ring mode was observed at 801 cm^{-1} (area3). However, there was some broadening in the peak at 3000-3500 cm^{-1}, which is indexed to CO vibration.

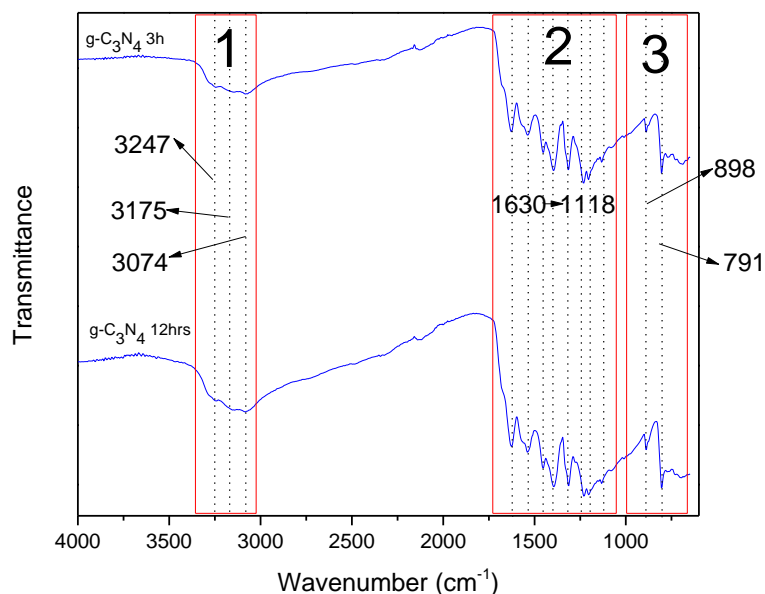**Figure 4.** FTIR spectrum of g-C$_3$N$_4$ samples obtained after 3 and 12 h of heating.

3.2 Optical properties of nanosheets

The UV-Vis diffuse reflectance spectroscopy (UV-Vis DRS) was conducted to assess the optical properties of the g-C$_3$N$_4$ samples. Fig. 5a illustrates the main absorption results for g-C$_3$N$_4$ heated for 3 and 12 h. The optical absorption edge of g-C$_3$N$_4$ heated for 3 occurs at 390 nm and then red shifts to a longer wavelength for g-C$_3$N$_4$ heated for 12 h, to 410 nm. The effect of a longer thermal oxidation treatment is consistent with the reported results.[29,30] Moreover, the g-C$_3$N$_4$12h sample was more efficient than the g-C$_3$N$_4$3h sample in absorbing near UV and visible range up to 470nm. The spectra exhibit a long absorption tail for the samples treated for 12 h, and this can be attributed to structural defects

90

formed in the sample treated for a longer time. The Tauc plot was used to calculate the optical band gap.[31] The Tauc plots (the curve of $(\alpha h\upsilon)^2$ versus E where E is the energy in eV and A is the absorption) are shown in Fig. 5b and 5c. The band gap value of g-C$_3$N$_4$ was calculated to be 2.7 eV for g-C$_3$N$_4$ heated for 3 and 12 h. The analysis of the band gap values shows that the main structure of g-C$_3$N$_4$ was present and dominant in all samples.
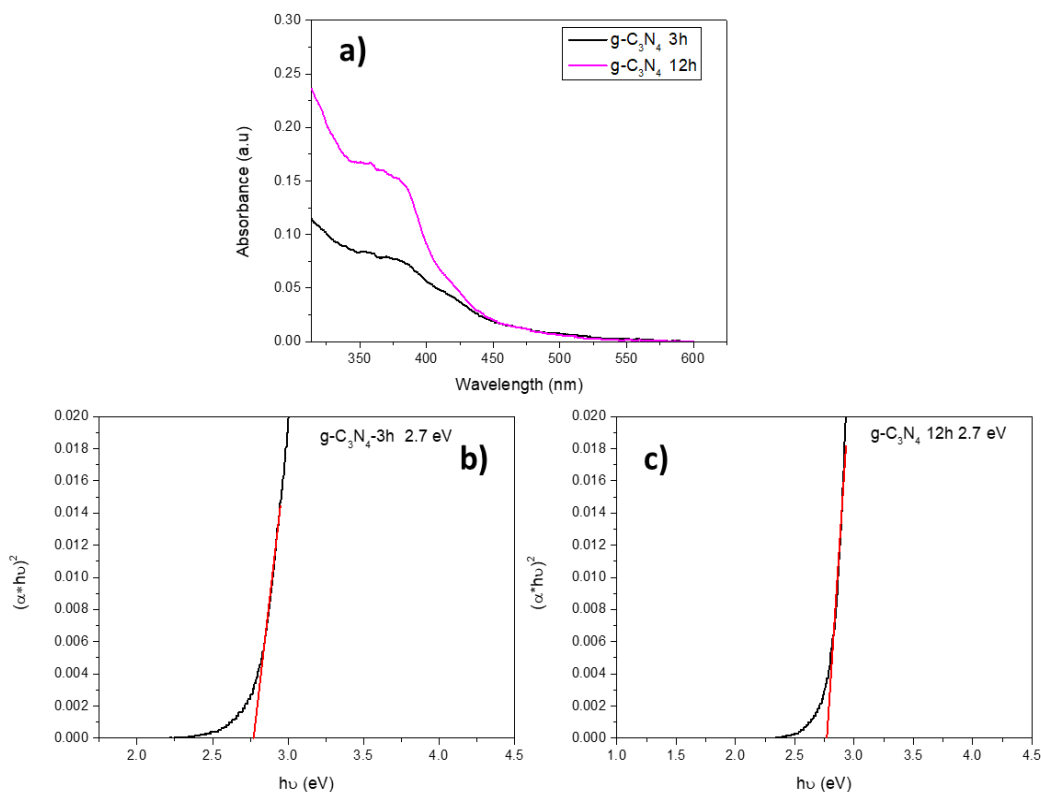

Figure 5. (a) The UV-Vis absorption spectra for g-C$_3$N$_4$ samples. (b) and (c) represent the Tauc graph with estimated band gap value for g-C$_3$N$_4$ samples.

Figure 6a showsthe chemical composition of the constituent elements of the g-C$_3$N$_4$, obtained by XPS analysis. The XPS spectra reveal that the main elements present were carbon, nitrogen and some oxygen. The high resolution spectra of carbon and nitrogen peaks are shown in Fig. 6b. The binding energies at 286.7, 288.4 and 289.2 eV are indexed to carbon from C-NH$_2$, C-N and C=N respectively, while the binding energies at 397.1, 397.1 and 400.3 eV are attributed to nitrogen from C=N- C, N-(C)$_3$ and C-N-H respectively. Moreover, some changes occurred for the carbon and nitrogen peaks after treating the sample up to 12 hours. Low intensity core level peaks were detected indicating the surface modification of the sample. Two peaks appear at binding energies 284.27 and 290.2 eV which could be attributed to C-C or C-H carbons while the other peak at 290.2 eV can be assigned to CO resulting from the etching process, and adsorbed on the sample surface [32-33]. This result is compatible with broadening observed in the FTIR result. For the nitrogen, the peak at binding energy 393.6 eV can be assigned to edge type N pyridinic which was reported previously for the sample prepared at higher energy [34-36]. The amounts of each element and the carbon to nitrogen ratio (C/N) (wt%) are shown in Table 1. There was a slight increase in the C/N ratio. This enhancement may indicate a carbon-rich surface which may enhance the photocatalytic activity by promoting charge carrier separation [37].
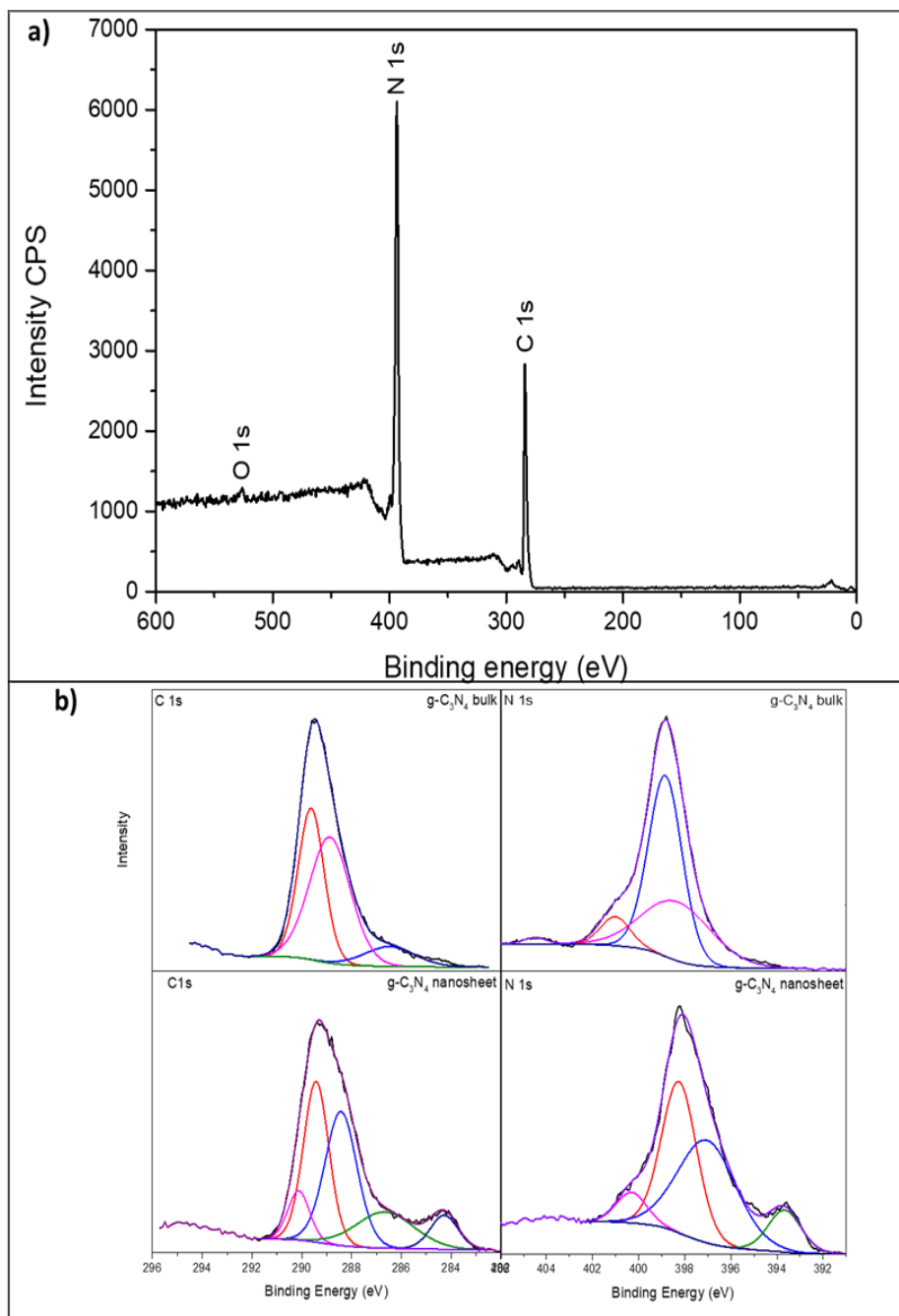
Figure 6. (a) The XPS survey of g-C$_3$N$_4$ and (b) comparison of high resolution spectra of C1s and N1s for the g-C$_3$N$_4$ 3h and g-C$_3$N$_4$ 12h .

Table 1. The amount of C, N, and O in different g-C$_3$N$_4$ samples.

XPS surface elemental analysis				
Content (%)	C	N	O	C/N
g-C$_3$N$_4$ 3h	42.23	56.92	0.65	0.74
g-C$_3$N$_4$ 12h	43.68	55.54	0.78	0.78

The photoluminescence emission (PL) spectra of as-obtained g-C_3N_4 samples are shown in Fig. 7. The PL measurement was performed at room temperature for the g-C_3N_4 3h and g-C_3N_4 12 h samples at excitation wavelengths of 360 nm. The main emission peak is located at about 450 nm for both samples. The emission peak resulted from the photo-generated electron-hole pairs process in the g-C_3N_4. Moreover, the emission intensity indicates the rate of photo generated electron-hole pairs. The spectra show that the g-C_3N_4 heated for 12 h had a higher intensity compared to that for the g-C_3N_4 heated for 3 h. The decrease in the intensity can be explained by the electron trapping process that occurs within the bulk material due to a crystal mismatch, which prevents electron-hole mobility. Moreover, the formation of nanosheets promoted the charge mobility in the g-C_3N_4 heated for 12 h.[38]
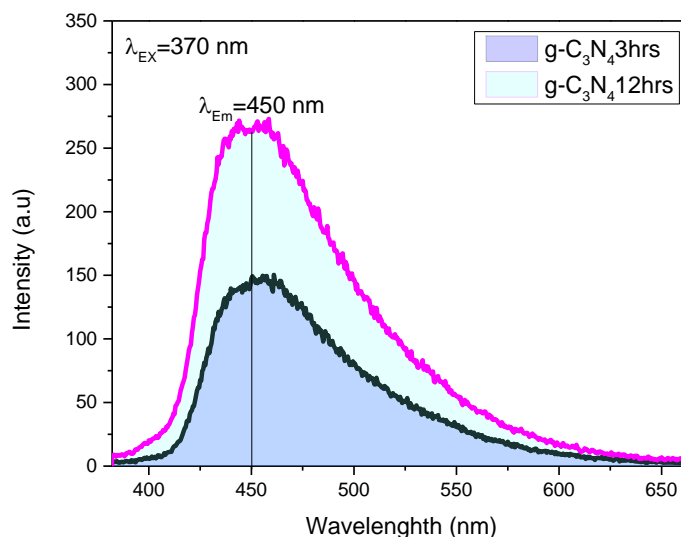

Figure 7. The comparison of photoluminescence (PL) spectra of g-C_3N_4 prepared at different thermal oxidation times.

3.3 Particles size and BET analysis

The reduction of g-C_3N_4 multilayered structure (bulk) to few-layered g-C_3N_4 nanosheets was followed by size particles analysis with the help of a particle sizer. The measurements were performed for both the sample heated for 3 hours and the sample heated for 12 hours. The particle size distributions are shown in Fig. 8a and 8b, the average particle sizes being 4967 and 1783 nm for g-C_3N_4 3h and g-C_3N_4 12h respectively. This decline in the particle size is attributed to the thermal oxidation etching process. Moreover, the BET surface area and porosity of the samples was analysed, with the result showing a type 3 shape of isotherms according to the IUPAC classification (Fig. 8c). This result indicates the occurrence of slightly mesoporous-like structure due to the aggregation of sheets to form the bulk g-C_3N_4, leaving pores in between.[39] The BET surface area was found to be 94.2435 and 94.2435 m^2/g, where the BJH adsorption surface area of pores was found to be around 123.0573 and 37.8759 m^2/g for g-C_3N_4 3h and g-C_3N_4 12h respectively. This decrease indicates the transformation of the multilayers of g-C_3N_4 3h (bulk) to a few layers of g-C_3N_4 nanosheets after 12h, where a significantly low amount of surface area was available for nitrogen adsorption due to the overlap of the single nanosheets [40].
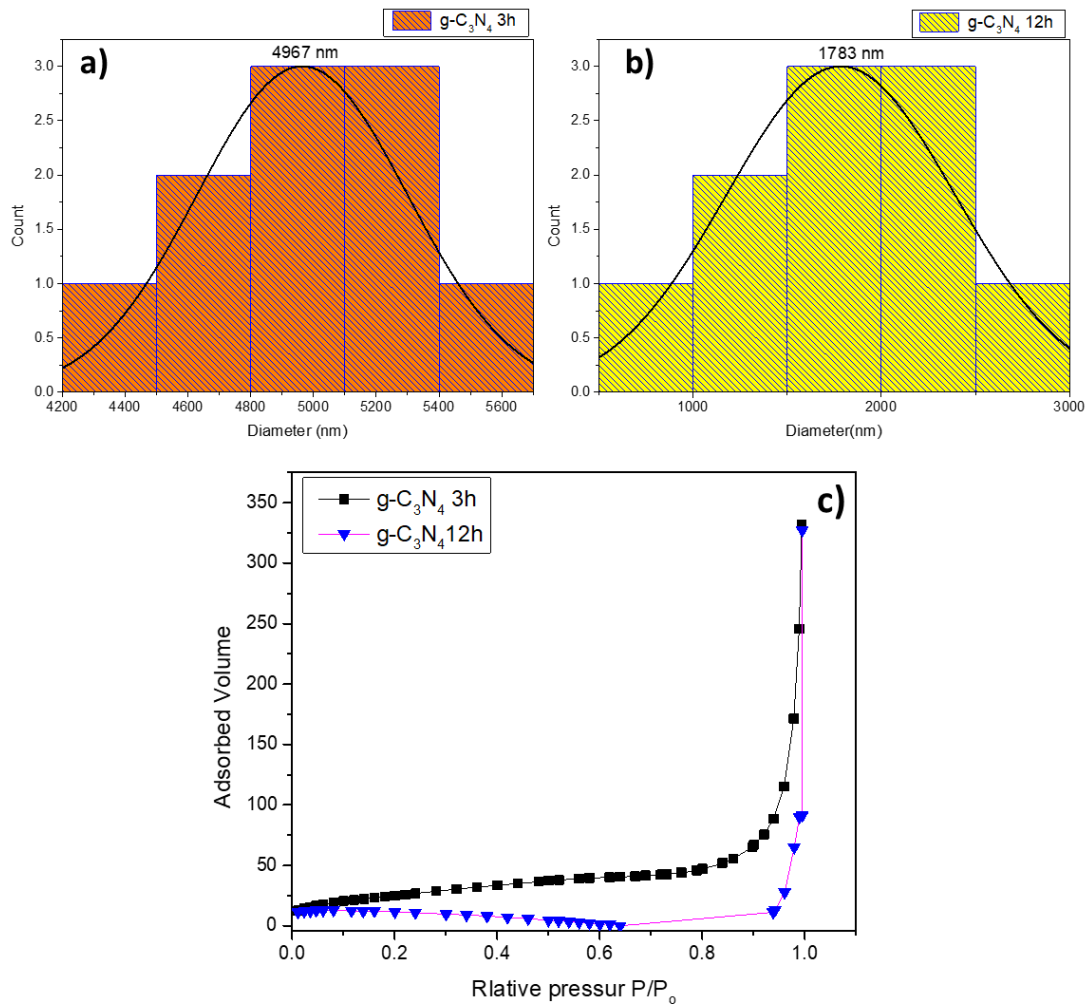
Figure 8. Histogram of corresponding particle size distribution (a) g-C$_3$N$_4$ 3h, (b) g-C$_3$N$_4$ 12h (c) BET surface area plot of g-C$_3$N$_4$ samples

3.4 Evaluation of the photocatalytic activity

Bisphenol A was chosen as a pollutant to determine the photocatalytic activity of the as-obtained catalysts on endocrine disrupting chemicals. Bisphenol A is often used as a model for hard degraded endocrine disrupting chemical pollutants. The performance of the g-C$_3$N$_4$ nanosheets was studied with the help of UV-Vis absorption spectra changes where the maximum absorptive energy is at 278 nm. Fig. 9a shows that the band intensity at 278 nm gradually declines with an increase in the irradiation time. These results indicate that Bisphenol A underwent degradation under the catalysis of g-C$_3$N$_4$. Fig. 9b shows a comparison of the photocatalytic degradation between g-C$_3$N$_4$ bulk and g-C$_3$N$_4$ nanosheets. Bisphenol A degraded faster using g-C$_3$N$_4$ heated for 12 h (around 60%) than with g-C$_3$N$_4$ bulk material (around 30%).

4. Conclusion

In this work, photocatalytic enhancement has been achieved for degradation of Bisphenol A (BPA) through g-C$_3$N$_4$ nanosheet photocatalysis, the nanosheet samples being obtained by direct heating of melamine followed by thermal oxidation etching for 12 h. The g-C$_3$N$_4$3h bulk material was obtained to conduct a comparison by performing the etching process for only three hours. Moreover, the g-C$_3$N$_4$12h nanosheet samples show very good photocatalytic activity under solar irradiation when compared to the bulk samples. This enhancement of the photocatalytic activity can be attributed to multiple factors such as the smaller particle size, carbon-rich surface and high surface area exhibited by the g-C$_3$N$_4$ nanosheets. Such g-C$_3$N$_4$ nanosheets have good potential for use in advanced water and wastewater treatment to eliminate endocrine disrupting chemicals under solar light irradiation or reduce them to a very low level.
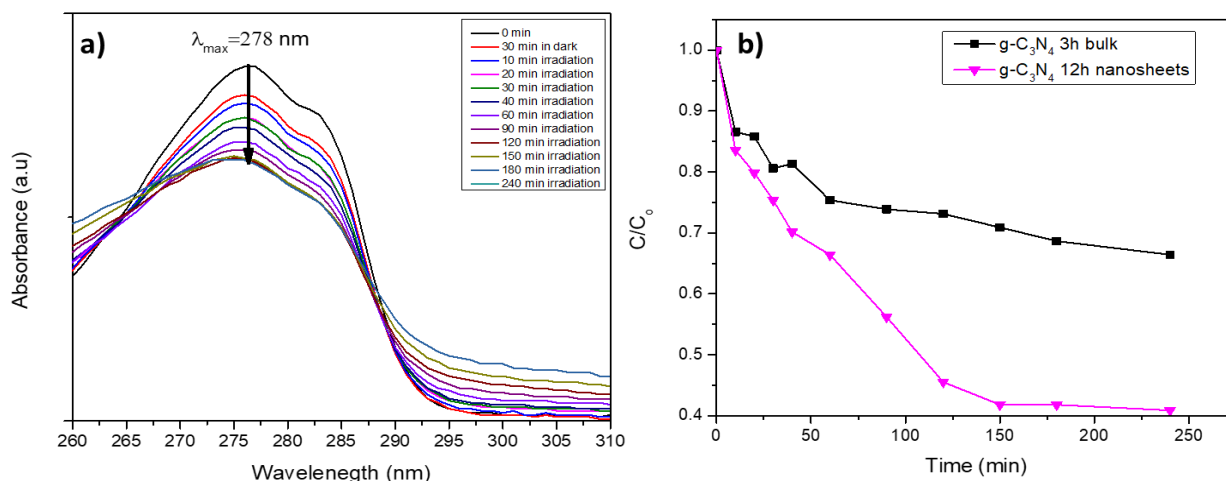
Figure 9. (a) Time-dependent UV-vis absorption spectra of Bisphenol A (10mg/L) degradation with g-C_3N_4 12 h nanosheets under solar light irradiation [catalyst dosage 100 mg, solution volume 250 ml, source of light solar] (b) Photocatalytic degradation of Bisphenol A with g-C_3N_4 prepared at different thermal oxidation time under solar light irradiation.

Conflict of interest

The authors declare no conflict of interest.

Acknowledgment

References

1. Ribeiroa, A.R., Nunesb, O.C., Pereiraa, M.F.R. and Silvaa, A.M.T. An overview on the advanced oxidation processes applied for the treatment of water pollutants defined in the recently launched Directive 2013/39/EU, *Environment International*. 2015, **75**, 33-51.
2. Sirés, I. and Brillas, E. Remediation of water pollution caused by pharmaceutical residues based on electrochemical separation and degradation technologies: A review, Environ. Int. 2012, **40**, 212-229.
3. Halling-Sørensen, B., Nielsen, S.N., Lanzky, P.F., Ingerslev, F., Lützhøft, H.C.H. and Jørgensen, S.E. Occurrence, fate and effects of pharmaceutical substances in the environment-A review, Chemospherem, 1998, **36**, 357-393.
4. Luo, Y., Guo, W., Ngo, H.H., Nghiem, L.D., Hai, F.I., Zhang, J., Liang, S. and Wang, X.C. A review on the occurrence of micro pollutants in the aquatic environment and their fate and removal during wastewater treatment, Sci. Total Environ. 2014, **474**, 473, 619-641.
5. Jurado, A., Vàzquez-Suñé, E., Carrera, J., de Alda, M.L., Pujades, E. and Barcelócd, D. Emerging organic contaminants in groundwater in Spain: A review of sources, recent occurrence and fate in a European context, Sci. Total Environ. 2012, **440**, 82-94.
6. Ioannidou, E., Ioannidi, A., Frontistis, Z., Antonopoulou, M., Tselios, C., Tsikritzis, D., Konstantinou, I., Kennou, S., Kondarides, D.I. and Mantzavinos, D. Correlating the properties of hydrogenated titania to reaction kinetics and mechanism for the photocatalytic degradation of bisphenol A under solar irradiation, Appl. Catal. B 2016, **188**, 65-76.
7. Kaneco, S., Rahman, M.A., Suzuki, T., Katsumata, H. and Ohta, K. Optimization of solar photocatalytic degradation conditions of bisphenol A in water using titanium dioxide, J. Photoch. Photobio A 163, 2004, 419-424.
8. Osterloh, F.E. Inorganic materials as catalysts for photochemical splitting of water, Chem. Mater. 2008, **20**, 35-54.

9. Chen, X., Shen, S., Guo, L. and Mao, S.S. Semiconductor-based photocatalytic hydrogen generation, Chem. Rev. 110, 2010, 6503-6570.

10. Kudo, A. and Miseki, Y. A heterogeneous photo catalyst material for water splitting, Chem. Soc. Rev. 38, 2009, 253-278.

11. Lang, X., Chen, X. and Zhao, J. Heterogeneous visible light photocatalysis for selective organic transformations, Chem. Soc. Rev. 2014, **43**, 473-486.

12. Bai, Y., Chen, T., Wang, P., Wang, L., Ye, L., Shi, X. and Bai, W. Size-dependent role of gold in g-C_3N_4/BiOBr/Au system for photocatalytic CO_2 reduction and dye degradation, Sol. Energ. Mat. Sol. C 157, 2016, 406-414.

13. Fresno, F., Portela, R., Suárez, S. and Coronado, J.M. Photocatalytic materials: recent achievements and near future trends, J. Mater. Chem, A2, 2014, 2863-2884.

14. Yu, J.C., Zhang, L., Zheng, Z. and Zhao, J. Synthesis and characterization of phosphated mesoporous titanium dioxide with high photocatalytic activity, Chem. Mater. 2003, **15**, 2280-2286.

15. Wang, X., Maeda, K., Thomas, A., Takanabe, K., Xin, G., Carlsson, J.M., Domen, K. and Antonietti1, M. A metal-free polymeric photocatalyst for hydrogen production from water under visible light, Nat. Mater. 2009, **8**, 76-82.

16. Al Marzouqi, F., Selvaraj, R. and Kim, Y. Rapid photocatalytic degradation of acetaminophen and levofloxacin using g-C_3N_4 nanosheets under solar light irradiation. Materials Research Express 2020, **6(12)**, 125538.

17. Al Marzouqi, F., Selvaraj, R. and Kim, Y. Shifting of the band edge and investigation of charge carrier pathways in the CdS/g-C_3N_4 heterostructure for enhanced photocatalytic degradation of levofloxacin. *New Journal of Chemistry* 2019, **43(25)**, 9784-9792.

18. Tian, N., Huang, H., He, Y., Guo, Y. and Zhang, Y. Novel g-C_3N_4/$BiIO_4$ heterojunction photocatalysts: synthesis characterization and enhanced visible light-responsive photocatalytic activity, RSC Adv. 4, 2014, 42716.

19. Wang, Y., Wang, X. and Antonietti, M. Polymeric graphitic carbon nitride as a heterogeneous organocatalyst: from photochemistry to multipurpose catalysis to sustainable chemistry, Angew. Chem. Int. Ed. 2012, **51**, 68-89.

20. Yan, S.C., Li, Z.S., Zou, Z.G. Photo degradation performance of g-C_3N_4 fabricated by directly heating melamine, Langmuir, 2009, **25**, 10397-10401.

21. Liu, J., Zhang, Y., Lu, L., Wu, G. and Chen, W. Self-regenerated solar-driven photocatalytic water splitting by urea derived graphitic carbon nitride with platinum nanoparticles, Chem. Commun. 2012, **48**, 8826-8828.

22. Al Marzouqi, F., Selvaraj, R. and Kim, Y. Thermal oxidation etching process of g-c3n4nanosheets from their bulk materials and its photocatalytic activity under solar light irradiation. Desalination and Water Treatment, 2018, **116**, 267-276.

23. Zhao, Y.C., Yu, D.L., Yanagisawa, O., Matsugi, K. and Tian, Y.J. Structural evolution of turbo static carbon nitride after being treated with a pulse discharge, Diam. Relat. Mater. 2005, **14**, 1700-1704.

24. Ma, H.A., Jia, X.P., Chen, L.X., Zhu, P.W., Guo, W.L., Guo, X.B., Wang, Y.D., Li, S.Q., Zou, G.T. and Zhang, G. High-pressure pyrolysis study of $C_3N_6H_6$: a route to preparing bulk C_3N_4, J. Phys. Condens. Matter. 14, 2002, 11269.

25. Liu, B., Qiao, M., Wang, Y., Wang, L., Gong, Y., Guo, T. and Zhao, X. Persulfate enhanced photocatalytic degradation of bisphenol A by g-C_3N_4 nanosheets under visible light irradiation. Chemosphere 2017, **189**, 115-122.

26. Chen, X., Zhang, L., Zhang, B., Guo, X. and Mu, X. Highly selective hydrogenation of furfural to furfuryl alcohol over Pt nanoparticles supported on g-C_3N_4 nanosheets catalysts in water, Sci. Rep. 6, 2016, 28558.

27. Yuan, X., Zhou, C., Jing, Q., Tang, Q., Mu, Y. and Du, A. Facile synthesis of g-C_3N_4 nanosheets/ZnO nanocomoosites with enhanced photocatalytic Activity in reduction of aqueous chromium(VI) under visible light, Nanomaterials 2016, **6**, 173.

28. Y. Guo, T. Chen, Q. Liu, Z. Zhang, Z. Fang, Insight into the enhanced photocatalytic activity of potassium and iodine Co doped graphitic carbon nitride photocatalysts, J. Phys. Chem. C 120, 2016, 25328-25337.

29. H.Li, X., Chen, J.S., Wang, X., Sun, J. and Antonietti, M. Metal-free activation of dioxygen by graphene/g-C_3N_4 nanocomposites: functional dyads for selective oxidation of saturated hydrocarbons, J. Am. Chem. Soc. 133, 2011, 8074-8077.

30. Zhang, Y., Mori, T., J.Ye. and Antonietti, M. Phosphorus-doped carbon nitride solid: enhanced electrical conductivity and photocurrent generation, J. Am. Chem. Soc. 132, 2010, 6294-6295.

31. Liu, J., Liu, Y., Liu, N., Han, Y., Zhang, X., Huang, H., Lifshitz, Y., Lee, S.T. and Zho, J. Metal-free efficient photocatalyst for stable visible water splitting via a two-electron pathway, Science 2015, **347**, 970-974.

32. B.R. Pistillo, K. Menguelti, D. Arl, F. Addiego, D. Lenoble; PRAP-CVD: how to design high conformal PEDOT surfaces, RSC Adv. 2017,**7**, 19117-19123.

33. Xiao, J., Xie, Y., Cao, H., Wang, Y., Guo, Z. and Chen, Y. Towards effective design of active nanocarbon materials for integrating visible-light photocatalysis with ozonation, Carbon 2016, **107,** 658-666.

34. Gammon, W.J., Kraft, O., Reilly, A.C. and Holloway, B.C. Experimental comparison of N(1s) X-ray photoelectron spectroscopy binding energies of hard and elastic amorphous carbon nitride films with reference organic compounds, Carbon 2003, **41**, 1917-1923.

35. Susi, T., Pichler, T. and Ayala, P. X-ray photoelectron spectroscopy of graphitic carbon nanomaterials doped with heteroatoms, Beilstein J. Nanotech. 2015, **6**, 177-192.
36. Yang, F., Kuznietsov, V., Lublow, M., Merschjann, C., Steigert, A., Klaer, J., Thomas, A. and Schedel-Niedrig, T. Solar hydrogen evolution using metal-free photocatalytic polymeric carbon nitride/CuInS$_2$ composites as photocathodes, J. Chem. Mater. A1, 2013, 407-6415.
37. Shi, A., Li, H., Yin, S., Liu, B., Zhang, J. and Wang, Y. Effect of conjugation degree and delocalized π-system on the photocatalytic activity of single layer g-C$_3$N$_4$, Appl. Catal. B-Environ. 2017, **218**, 137-146.
38. Ge, L., Zuo, F., Liu, J., Ma, Q., Wang, C., Sun, D., Bartels, L. and Feng, P. Synthesis and efficient visible light photocatalytic hydrogen evolution of polymeric g-C$_3$N$_4$ coupled with CdS quantum dots, J. Phys. Chem. C 116, 2012, 13708-13714.
39. Dong, F., Li, Y., Wang, Z.Y., Ho, W.K. Enhanced visible light photocatalytic activity and oxidation ability of porous graphene-like g-C$_3$N$_4$ nanosheets via thermal exfoliation, Appl. Surf. Sci. 2015, **358**, 393-403.
40. McAllister, M.J., Li, J.-L., Adamson, D.H., Schniepp, H.C., Abdala, A.A., Liu, J., Herrera-Alonso, M., Milius, D.L., Car, R., Prud'homme, R.K. and Aksay, I.A. Single Sheet Functionalized Graphene by Oxidation and Thermal Expansion of Graphite, Chem Mater. 2007, **19**, 4396-4404.